http://dx.doi.org/10.5935/0100-4042.20140246 *Quim. Nova,* Vol. 37, No. 9, 1446-1452, 2014

MODULATING THE ELECTRONIC STRUCTURE OF AMINO ACIDS: INTERACTION OF MODEL LEWIS ACIDS WITH ANTHRANILIC ACID

Tareq Irshaidat*
Department of Chemistry, Al-Hussein Bin Talal University, Ma'an, Jordan

Recebido em 06/03/2014; aceito em 19/06/2014; publicado na web em 05/09/2014

On the basis of theoretical B3LYP calculations, Yáñez and co-workers (*J. Chem. Theory Comput.* **2012**, *8*, 2293) illustrated that beryllium ions are capable of significantly modulating (changing) the electronic structures of imidazole. In this computational organic chemistry study, the interaction of this β-amino acid and five model Lewis acids (BeF^{1+}, Be^{2+}, AlF_2^{1+}, AlF^{2+}, and Al^{3+}) were investigated. Several aspects were addressed: natural bond orbitals, including second order perturbation analysis of intra-molecular charge delocalization and the natural population analysis atomic charges; molecular geometries; selected infrared stretching frequencies (C–N, C–O, and N–H), and selected ^{1}H-NMR chemical shifts. The data illustrate that this interaction can weaken the H–O bond and goes beyond strengthening the intra-molecular hydrogen bond (N…H–O) to cause a spontaneous transfer of the proton to the nitrogen atom in five cases generating zwitterion structures. Many new features are observed. Most importantly, the zwitterion structures include a stabilizing hydrogen bond (N–H…O) that varies in relative strength according to the Lewis acid. These findings explain the experimental observations of α-amino acids (for example: *J. Am. Chem. Soc.* **2001**, *123*, 3577) and are the first reported fundamental electronic structure characterization of β-amino acids in zwitterion form.

Keywords: amino acid; anthranilic acid; zwitterion; hydrogen bond; NBO.

INTRODUCTION

The zwitterion is an important concept in organic and biochemistry. Owing to its importance, hundreds of publications have discussed its characteristics. Zwitterions are particularly important for describing the equilibrium structures of amino acids, one of the most important building blocks in all living systems. Understanding the structure of a biomolecule to predict its function is very important in biology and chemistry. Because of the enormous number of factors affecting biomolecular structure, this is a highly multifaceted task. By investigating model systems in a controlled simple environment, the influence of the effects can be evaluated individually. Therefore, the structure of many biomolecules has been studied in the absence of environmental effects in numerous gas-phase conditions.[1-15]

It is known that the stability of a zwitterion in gas phase depends on the basicity and acidity of the involved functional groups. For arginine, with its strongly basic guanidine group, calculations indicated that the zwitterion is nearly as stable as the neutral form.[16] In addition, several aggregates of arginine that are bound by salt bridges were discovered. Quadrupole ion-trap mass spectrometry and *ab-initio* calculations provided evidence for the stability of arginine in the zwitterion state, interacting with either a cation or anion.[17] Many other studies confirmed that the zwitterion form of an amino acid can be stabilized by specific interactions with nearby ions or molecules.[18-30] In line with these observations, on the basis of B3LYP calculations, Yáñez and co-workers[31] concluded that the interaction of beryllium salts with imidazole may cause a significant increase in hydrogen bond strength. This indicates that a metal ion competes for the electron density of the carboxylate group, which in turn increases polarization of the H–O bond and consequently weakens it causing a decrease in the energy of the anti-bonding orbital of the H–O bond. Therefore, an efficient overlapping between the lone pair orbital of the nitrogen atom and the anti-bonding orbital (of H–O) can occur, implying much stronger hydrogen bonding. Under this effect, the proton may transfer to the nitrogen atom forming a more stable bonding status.

The zwitterion of β-amino acids has not received any significant attention. Thus, the purpose of this work is to investigate the previous observations and facts in an attempt to shed light on the fundamental electronic structure feature of β-amino acids in the zwitterion form. Considering anthranilic acid for this study was originally motivated by the important roles it plays in cell biology.[32-49] Previously, it was used[50-53] as a model compound to study several physical organic chemistry features. As a continuation of previous efforts toward a better understanding of the electronic structure of β-amino acids and anthranilic acid, here we examine the consequences of the interaction with representative Lewis acids (BeF^+ (Be1), Be^{2+} (Be2), AlF^{2+} (Al1), AlF^{2+} (Al2), and Al^{3+} (Al3)) and investigate how such effectors can modulate (change) the electronic structure. This beta-amino acid is the amino acid of interest in this study; however, for comparison, the 4-aminobenzoic acid in the zwitterion form (4-AAZ) (Figure 1) is used as a model to represent a pure zwitterion that does not contain the N–H1…O1 interfering interaction.

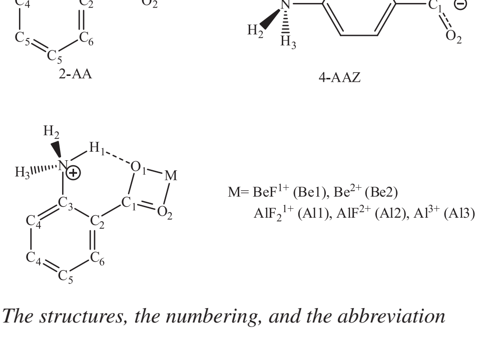

2-AA

4-AAZ

M= BeF^{1+} (Be1), Be^{2+} (Be2)
AlF_2^{1+} (Al1), AlF^{2+} (Al2), Al^{3+} (Al3)

***Figure 1.** The structures, the numbering, and the abbreviation*

---

*e-mail: tirshaidat@yahoo.com

COMPUTATIONAL METHOD

All structures were optimized using the hybrid functional B3LYP[54] and the 6-31G(d) basis set.[55] The frequency calculations indicated that all resulting structures were true minima because all frequencies were real (positive values). Then, single point calculations were performed using the 6-311+G(2d,p) basis set.[56,57] The standard natural bond orbital (NBO) method[58] was used to calculate the natural population analysis (NPA) charges and to perform the second order perturbation analysis. The latter provides the values of the intra-molecular charge delocalization energies (E2), which gives a qualitative evaluation for the relative interaction between an electron pair (bonding or non-bonding pair) and an empty orbital (s-, p-, d-orbital, or anti-bonding orbital). The nuclear magnetic resonance chemical shifts were calculated using the GIAO[59] scheme. Tetramethylsilane (TMS) was considered the reference for both hydrogen and carbon chemical shifts. All the above calculations were performed using a Gaussian 03 suit of programs.[60] The harmonic oscillator model of aromaticity (HOMA) was calculated based on recommended literature procedure.[61] For example, in a benzene molecule, when the aromatic character is 100% then the p-orbitals overlap perfectly and the HOMA value is 1, and when the aromatic character is 0%, the double bonds in the ring are completely localized and the HOMA value is zero. Most known aromatic molecules have values ranging between the two limits (0.00–1) depending on the interaction of substituents with the ring; a larger interaction usually causes more disturbance of the overlapping p-orbitals and consequently a loss in aromatic character. The ChemCraft graphics interface was employed in all computations to generate the input and to read the output files. Examples from recent literature show that the adopted level of theory can produce satisfactory results.[62-70]

RESULTS AND DISCUSION

The second order perturbation analysis

Three types of intra-molecular interactions are presented in Table 1 based on the two computational procedures, B3LYP/6-31G(d) and B3LYP/6-311+G(2d,p)//B3LYP/6-31G(d). The first interaction is the hydrogen bond between the lone pair of O1 and the antibonding orbital of the N–H1 bond. However, in case of 2-AA it is from the lone pair of N to the antibonding orbital of the H1–O1 bond. The second interaction is between the lone pair of O1 and the ϖ^* orbital of C1=O2. The third is the interaction between the lone pair of O1 and the empty p-orbital on C1. The empty p-orbital results from moving the ϖ-electron pair of C1=O2 to become completely localized on O2. Some values could not be observed, which means that the related level of theory predicts that such an interaction does not exist. The obtained values show some variations; however, they are qualitatively consistent and give the same description of the whole picture, as in the following analysis.

Previously, we investigated the neutral form of anthranilic acid and estimated the hydrogen bond strength based on a comparison with a model equilibrium isomerization reaction and investigated the second order perturbation analysis of the NBOs.[53] The estimated hydrogen bond energy is close to 10.7 kcal/mol, which makes it the strongest neutral (N…H–O) hydrogen bond encountered that it is not a resonance assisted hydrogen bond (RAHB). This hydrogen bond is associated with a 25.66 kcal/mol of charge delocalization energy (B3LYP/6-311+G(2d,p)). Table 1 shows that the strongest (O1…H1–N) is predicted to be in Be1 (B3LYP/6-311+G(2d,p) = 28.81 kcal/mol). Qualitatively, the values indicate that the hydrogen bond in Be1 is also strong. On the other hand, the increase in the positive charge of the Lewis acid decreases the ability of the O1 atom to delocalize electron density toward the anti-bonding orbital of N–H1, causing relatively weaker hydrogen bonds. Evaluating the hydrogen bond strength has been the subject of several studies.[71-73] G. Gilli[73] summarized and illustrated that the energy of a strong hydrogen bond is in the 6.8–11.5 kcal/mol range, which supports classifying the N…H–O hydrogen bond strength in anthranilic acid and the O…H–N hydrogen bond in Be1 as strong hydrogen bonds. Examples of stronger RAHBs are malonaldehyde[74] (12.4 kcal/mol) and acetylacetone[75] (12.0 kcal/mol), in which the resonance in the O=C–C=C–OH segment is an important factor in strengthening the intra-molecular hydrogen bond.

It appears that the carboxylate group may exist in two resonance forms, (–)O1–C1=O2 and (–)O1–C1(+)–O2(–). The electronic structures of 2-AA contain the N…H–O1–C1=O2 form based on absence of any appreciable O1→C1 (0.00 kcal/mol) delocalization, which indicates that the N…H–O1–C1(+)–O2(–) resonance form does not exist. The values in parentheses are the ratios between the values of the O1→C1=O2 and the O1→C1 interactions. This ratio is an estimation for the relative population of the two resonance forms (B3LYP/6-311+G(2d,p) calculations), (−)O1–C1=O2 with respect to (−)O1–C1(+)–O2(−). It is obvious that the population in Be1, Be2, Al1, and Al2 is similar to that observed for 4-AAZ. The calculated ratios illustrate that the (−)O1–C1(+)–O2(−) resonance form is dominant, which is the first characterized case of its type in the literature.

The data that is presented in Table 2 are the total energies of the interactions between N–H2 and N–H3 with the anti-bonding orbitals located on the C2–C3–C4 part of the benzene ring. These interactions indicate that hyper-conjugation exists in all these structures. To best

Table 1. The charge delocalization energies (E(2); kcal/mol). The value between parentheses is the ratio between the O1→ C1=O2 and the O1→ C1 interaction energies

Structure	Interaction	6-31G(d)	6-311+G(2d,p)[a]
Be1	O1→ N-H1	34.72	28.81
	O1→ C1=O2	14.74 (0.107)	14.68 (0.115)
	O1→ C1	137.46	128.2
Be2	O1→ N-H1	8.73	5.69
	O1→ C1=O2	79.29	11.60 (0.115)
	O1→ C1	-	101.01
Al1	O1→ N-H1	28.68	22.77
	O1→ C1=O2	14.12 (0.105)	13.41 (0.107)
	O1→ C1	133.94	125.51
Al2	O1→ N-H1	8.81	5.56
	O1→ C1=O2	83.82	4.64 (0.045)
	O1→ C1	-	102.63
Al3	O1→ N-H1	3.34	1.64
	O1→ C1=O2	75.85	73.25
	O1→ C1	-	-
2-AA	N→ O1-H1	20.55	16.31
	O1→ C1=O2	49.70	48.74
	O1→ C1	-	-
4-AAZ	O1→ N-H1	0.00	0.00
	O1→ C1=O2	23.31 (0.098)	23.72 (0.111)
	O1→ C1	238.93	214.58

[a]Based on B3LYP/6-311+G(2d,p)//B3LYP/6-31G(d) calculations.

Table 2. The total charge delocalization energies (kcal/mol) of the interactions between each of the N-H2 and N-H3 bonds with the anti-bonding orbitals located on the C2-C3-C4 part of the benzene ring

Structure	6-31G(d)	6-311+G(2d,p)[a]
Be1	5.56	5.56
Be2	6.77	6.52
Al1	5.54	5.54
Al2	6.76	6.52
Al3	3.31	2.90
2-AA	8.56	8.62
4-AAZ	4.86	4.71

[a]Based on B3LYP/6-311+G(2d,p)//B3LYP/6-31G(d) calculations.

of our knowledge, these intra-molecular stabilizing interactions are the first reported hyper-conjugation cases between N–H and the anti-bonding orbitals of an aromatic ring. The values indicate that the interaction is of moderate strength with respect to the other non-covalent interactions. The effect of this interaction on the N…H–O hydrogen bond strength cannot be decomposed and quantified numerically. However, it can be shown quantitatively that donating an electron density from the N–H bonds would decrease the electron density on nitrogen and consequently would cause a decrease in the hydrogen bond strength.

Molecular geometries

We made many attempts to optimize the molecular structure of a zwitterion of 2-aminobenzoic acid; unfortunately, all resulted in optimization of the neutral structure. Therefore, the calculation of 4-aminobenzoic acid provides idea clue regarding the reason behind the impossibility of optimizing the zwitterion form of 2-aminobenzoic acid. We have found that converting 4-aminobenzoic acid to the zwitterion costs 66.23kcal/mol (B3LYP/6-311+G(2d,p)), a high price for the process.

Bonding to the metal cation (Figure 2) caused a significant distortion in the bond lengths of C1–O1 and C1–O2 with respect to 2-AA and 4-AAZ (Table 3). In the five metal-containing structures, the C1–O1 bond length became less than that of 2-AA. This indicates that O1 delocalizes part of its electron density towards the C1–O2 double bond, which increases the overlap and decreases the bond length. On the other hand, all C1–O2 bond lengths are larger than that of 2-AA, which is consistent with the changes in C1–O1. Therefore, it is generally inferred that bonding of the carboxylate group to the metal ion can cause an increase in the O1–C1 bond order and a decrease in the C1–O2 bond order (based on the O1–C1=O2↔O1=C1–O2 representation of charge delocalization). However, none of the metal-containing structures reach the ideal delocalization that is observed in 4-AAZ, in which each of the O1–C1 and the C1–O2 bonds has a bond order nearly equal to 1.5. This is attributed to the N–H1…O1 hydrogen bond that exists between H1 and O1; it is sufficiently strong to cause partial localization of the electron density of O1.

The C1–C2 bond length in the five metal-containing models (1.48 Å) is less than that in 2-AA and 4-AAZ, which is a result of the formation of the new N-H1…O1 hydrogen bond. This observation qualitatively supports the NBO analysis result, which showed that this non-covalent interaction could cause noticeable geometrical changes.

The observed data of the benzene ring illustrate that the bond lengths did not change systematically. However, after calculating the HOMA values of each structure, the changes in the overlap between the p-orbitals became clearer. The calculated values for Be1, Al1, and 2-AA are the same, which means that the zwitterion structure of Be1 and Al1 does not include any change in the aromatic overlapping with respect to 2-AA. On the other hand, the other Lewis acids (Be2, Al2 and Al3) affected the geometry of the benzene ring significantly. In these three cases, the aromatic character decreased by approximately 8% in Be2 and Al2 and by 16% in Al3 with respect to 2-AA (Figure 3). On the other hand, the HOMA value of 4-AAZ increased to 0.98. Therefore, despite the metal not being directly bonded to the benzene ring, it is inferred that the relative charge deficiency of the Lewis acid (Be1 and Al1 compared to Be2, Al2 and Al3) is a powerful factor that can cause noticeable distortion in the structural features of the organic skeleton by a cumulative effect transferring through the sigma bonds.

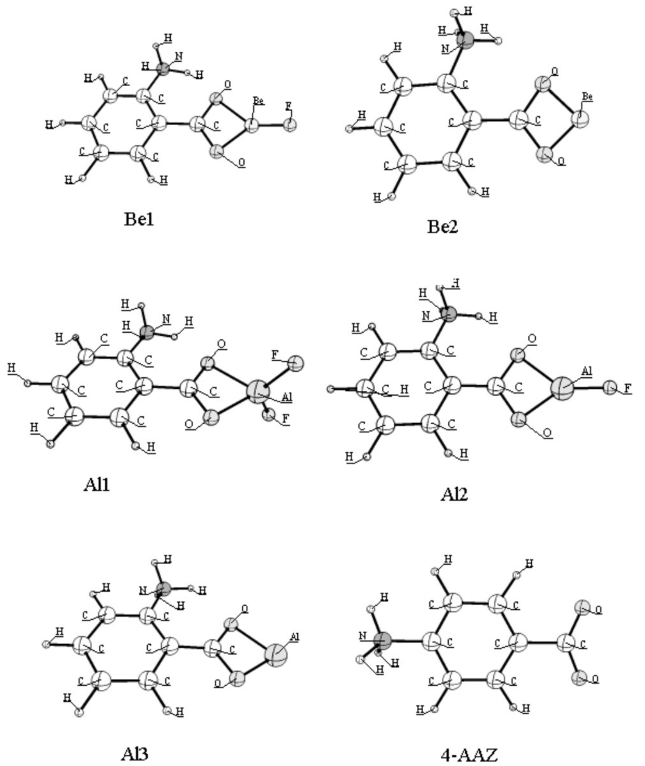
Be1 Be2

Al1 Al2

Al3 4-AAZ

***Figure 2.** The optimized structures of the five models and 4-AAZ*

A significant change is observed in the N–H1 bond length, which decreases with the increase in the charge of the Lewis acid. In addition, the observed decrease in N–H1 bond length is accompanied by the increase in the O1…H1 distance. However, the difference when the charges are (+2) and (+3) is small. These observations indicate that the order of the hydrogen bond strength (N–H1…O1) is Be1, Al1 > Be2, Al2 > Al3, which is consistent with the results obtained by the second order perturbation analysis (Table 1).

On the other hand, with regard to the length of the N-H(H2 and H3) bonds, only the values of Be1 and Al1 are closer to those of 4-AAZ. In general, it is obvious that the values of the N–H(2, 3) bond lengths increase with the increase in charge. To show the effect of metal ions on the electronic structure of the amino acid in a simplified manner, the relationship between the N–H2 bond length and the charge of the aluminum Lewis acids (AlF_2= +1, AlF= +2, and Al= +3) is presented in Figure 4. As shown in Figure 4, the relationship is linear. These observations are consistent with the conclusions presented by Yáñez and coworkers that interactions with metal ions can modulate a hydrogen bond and electronic structure properties.

In the carboxylate group, the change in C1–O2 bond length is gradual and a function of the Lewis acid charge. In contrast, the change in C1–O1 is not systematic, which may be attributed to the interfering effect of the $–NH_3^+$ group. The decrease in the hydrogen

Table 3. The geometrical parameters; bond lengths (Å) and angles (degrees)

Parameter	Be1	Be2	Al1	Al2	Al3	2-AA	4-AAZ
C1-O1	1.300	1.335	1.301	1.325	1.323	1.347	1.249
C1-O2	1.268	1.308	1.270	1.305	1.311	1.212	1.250
C1-C2	1.470	1.430	1.471	1.433	1.443	1.511	1.564
C2-C3	1.408	1.424	1.408	1.424	1.418	1.411	-
C3-C4	1.385	1.377	1.384	1.378	1.405	1.399	-
C4-C5	1.400	1.410	1.400	1.409	1.411	1.394	-
C5-C6	1.396	1.395	1.395	1.395	1.395	1.396	-
C6-C7	1.393	1.391	1.393	1.391	1.411	1.391	-
C7-C2	1.403	1.416	1.403	1.416	1.433	1.401	-
HOMA	0.96	0.88	0.96	0.88	0.81	0.96	0.98
C3-N	1.490	1.494	1.490	1.494	1.489	1.435	1.501
N-H1	1.055	1.034	1.052	1.034	1.033	1.817	1.026
N-H2	1.028	1.032	1.028	1.032	1.037	1.020	1.028
N-H3	1.028	1.032	1.028	1.032	1.038	1.017	1.028
O1…H1	1.699	1.942	1.712	1.941	2.110	0.990	-
O1…N	2.628	2.787	2.632	2.781	2.892	2.671	-
H1NC3C2	0.0	0.0	0.0	0.0	11.1	19.6	0.1
O1C1C2C3	0.0	0.1	0.0	0.0	6.3	14.8	0.0

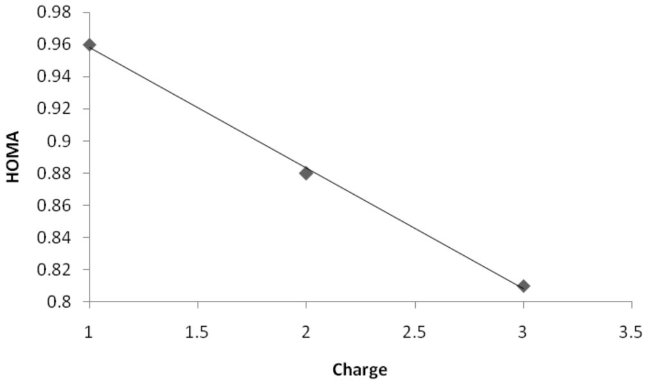

Figure 3. *A graph presenting the relationship between the charge of the Lewis acid and the HOMA values in Al1, Al2, and Al3*

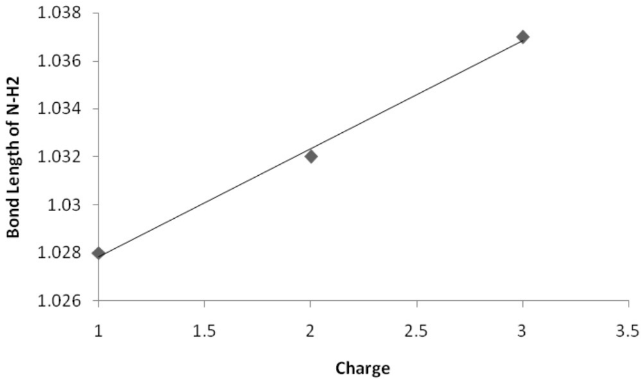

Figure 4. *A graph presenting the relationship between the charge of the Lewis acid and the bond length of N-H2 in the Al1, Al2, and Al3 structures*

bond is accompanied by a systematic increase in the distance between O1 and N. Accompanying this, the H1–N–C3–C2 and O1–C1–C2–C3 dihedral angles change in Al3, which also supports the previous conclusion that the hydrogen bond vanishes in this case.

NPA charges

The atomic charges are useful in evaluating the electronic structure. The group charges were calculated and are presented in Table 4. The calculated charge of the $CO_2M(F)$ moiety increases by increasing the charge of the Lewis acid, and minimum values are noticed for Al1 and Be1. The $CO_2M(F)$ segment charges of Be2, Al2, and Al3 were expected to be (1+) and (2+); however, the calculated values are less. This indicates that the benzene ring donates a negative charge to this moiety through the conjugated π-system, which is given by the entries for Ph↔CO2 (Table 4). The arrow under each value shows the direction of the donation. As can be seen, in both Be1 and Al1, the $CO_2M(F)$ group donates only a small negative charge to the phenyl ring. Note that this donation is through the sigma bond (a sigma bond polarization) rather than through the ϖ-system. In 2-AA, the donated amount is 0.016e, and in case of 4-AAZ it is a much higher value (0.314e).

In the same manner, the calculated charge of $-NH_3^+$ is less than one positive charge, which indicates that the benzene ring donates an electron density to nitrogen through the sigma bond. The donated values can be seen in the entries for C→N (Table 4). Even in the case of 2-AA, nitrogen drags an electron density because of the electronegativity difference. Therefore, correcting the charge values in the entries of C→N to the value of 2-AA produced the withdrawn electron density amount as a result of protonation (in parentheses). The corrected charge values indicate that the amount of polarization in the C–N bond is large. This result is consistent with the bond length changes of the C–N bond in the zwitterion structure and 2-AA (Table 3).

Taking the total charge (T.C.) of each structure and the charges of the $CO_2M(F)$ and the $-NH_3^+$ moieties into consideration, the charge of the phenyl ring can be calculated. In each of the metal-containing structures, the phenyl ring carries a positive charge significantly larger than that carried by the phenyl ring in 4-AAZ. The smallest amount of positive charge is noticed for Be1 and Al1 (0.327 and 0.343, respectively). This large bond polarization explains the very low stability of the zwitterion structure of anthranilic acid.

Selected infrared stretching vibrations and ^1H-NMR chemical shifts

Table 5 presents selected infrared stretching vibrations. The data of the C3–N bond indicate that formation of the zwitterion in the five

Table 4. The natural population charge analysis (T.C. refers to the total charge)

	Be1	Be2	Al1	Al2	Al3	2-AA	4-AAZ
$CO_2M(F)$	0.02	0.783	0.003	0.783	1.352	0.016	-0.686
NH_3	0.653	0.693	0.657	0.695	0.736	-0.080	0.623
T.C.	1	2	1	2	3	Zero	Zero
Ph	0.327	0.524	0.340	0.522	0.912	0.064	0.063
C→N	0.347e	0.307e	0.343e	0.305e	0.264e	0.080e	0.377e
	(0.267)	(0.227)	(0.263)	(0.225)	(0.184)	(0.000)	(0.297)
Ph↔CO2	0.020e	0.217e	0.003e	0.217e	0.648e	0.016e	0.314e
	←	→	←	→	→	←	←

Table 5. The selected infrared stretching frequencies (cm^{-1}). The small letter (s) refers to symmetric stretching and (as) refers to anti-symmetric stretching

	Be1	Be2	Al1	Al2	Al3	2-AA	4-AAZ
C3-N	809	796	808	809	790	843	755
C1-O1	1469	1384	1458	1390	1352	1139	1326 (O1/2; s)
C1-O2	1647	1404	1641	1410	1368	1840	1779 (O1/2; as)
N(O)-H	2977	3316	3023	3315	3294	3366	3372
	(H1)	(1,2,3 s)	(H1)	(1,2,3 s)	(1,2,3 s)	O1-H1	(1,2,3 s)
	3411	3392	3410	3392	3356	3478	3443
	(2,3 s)	(1/2,3 as)	(2,3 s)	(1/2,3 as)	(2/3 as)	(2,3 s)	(2/3 as)
	3468	3423	3466	3423	3388	3574	3479
	(2/3 as)	(2/3 as)	(2/3 as)	(2/3 as)	(1/2,3 as)	(2/3 as)	(1/2,3 as)

metal-models is weaker than in 2-AA and that the weakest exists in 4-AAZ. This result is consistent with the C3–N bond lengths (Table 3); the values of 2-AA and 4-AAZ are 1.435 and 1.501 Å, respectively. In the five models, a systematic change is observed in the C1–O1 and C1–O2 stretching frequencies, and the values indicate that both bonds become weaker by increasing the positive charge. This implies that as the Lewis acid becomes more electron deficient, it withdraws more electron density from the two oxygen atoms, which in turn decreases the electron density that exists in the parallel p-orbitals of the carboxylate group leading to a lower bond order and weaker bonds. This smooth continuous change in the C1–O1 and C1–O2 stretching frequencies is evident in Figure 5. The symmetry that exist in 4-AAZ causes an overlap; symmetric stretching appears at 1326 cm^{-1}, and anti--symmetric stretching appears at 1779 cm^{-1}. On the other hand, 2-AA has very different frequencies. C1–O1 stretches at 1139 cm^{-1}, which is characteristic for a single C–O bond, and the stretching frequency of C1–O2 in 2-AA appears at 1840 cm^{-1}, corresponding to a double bond.

The other important stretching vibration is the N–H or O–H stretching. In 2-AA, the O1–H1 bond stretches separate from the two N–H bonds at 3366 cm^{-1}. The two N–H bonds stretch in two modes. The first is a symmetric stretching that occurs at 3478 cm^{-1} and the second is an anti-symmetric stretching that appears at 3574 cm^{-1}. In 4-AAZ, the N–H bonds are nearly identical in strength and stretch in three modes. The first appears at 3372 cm^{-1} as a symmetric stretching, and the second is anti-symmetric and appears at 3479 cm^{-1} (N–H1 versus N–H2 and N–H3). The third is also anti-symmetric stretching that involves N–H2 and N–H3 and occurs at 3443 cm^{-1}. This indicates that N–H1 is different from the other two N–H bonds. On the other hand, unique vibrational modes are seen in Be1 and Al1. In both structures, the N–H1 bond stretches separately and at lower frequency than that of N–H2 and N–H3. In addition, N–H2 and N–H3 are related in symmetric and anti-symmetric vibrations. This demonstrates that N–H1 is considerably affected by the hydrogen bond with O1, which means that the N–H1 bond is weaker than the other two N–H bonds.

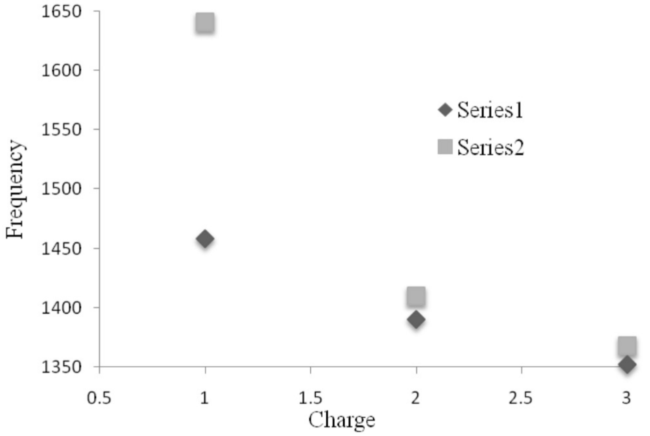

Figure 5. *A graph presenting the relationship between each of C1-O1 (series 1) and C1-O2 (series 2) stretching frequencies and the charge of the Al1, Al2, and Al3 model structures*

The most important chemical shift (Table 6) is that of H1. In 4-AAZ, it resonates at 4.7 ppm in the absence of hydrogen bonding. In 2-AA, the value indicates that H1 is considerably deshielded. The deshielding is due to two factors. The first is the polarization in the O1–H1 bond, which is greater than that in the N–H1 bond. The second is the N…H1–O1 hydrogen bond, which is known to cause considerable deshielding. Compared with the above two cases, the five metal-containing structures show resonance values between

Table 6. The selected ^{1}H-NMR chemical shifts (ppm)

	Be1	Be2	Al1	Al2	Al3	2-AA	4-AAZ
H1	11.2	7.9	11.0	7.9	5.8	12.0	4.7
H2	5.1	6.1	5.2	6.1	5.8	3.3	5.6
H3	5.1	6.1	5.2	6.1	4.9	3.5	5.6

4.9–12.0 ppm. It is obvious that there is systematic decrease in the chemical shift of H1. This indicates that the hydrogen bond decreases as the charge of the Lewis acid increases, which is consistent with the previous analyses.

CONCLUSION

The energy calculations for 4-aminobenzoic acid indicate that zwitterion formation in the structure of 2-aminobenzoic acid costs more than 60 kcal/mol, which explains why optimizing the zwitterion structure of 2-aminobenzoic acid (anthranilic acid) is not a straightforward task. The structural parameters show that bonding of the metal ions to the carboxylic acid group causes transfer of the H1–O1 proton to the nitrogen atom. The intra-molecular stabilizing charge delocalization interactions, the atomic charges, the infrared frequencies, and the NMR chemical shift data confirm that the optimized structures of the five models simulate the zwitterion structure of the β-amino acid. The analyses indicate that the zwitterion structure of anthranilic acid is best represented by Be1 and Al1 owing to the milder effect of the BeF(+) and AlF2(+) positive charges.

The second-order perturbation analysis of the intramolecular interactions illustrates that the structures of Be1 and Al1 include valuable hydrogen bonds between N–H1 and O1. Moreover, the analysis demonstrates that all the studied structures include unique cases of hyper-conjugation between the sigma bonds of N–H2/3 and the anti-bonding orbitals located on the C2–C3–C4 segment of the benzene ring. To the best of our knowledge, this is the first example of this type in the literature. The energy values of this interaction indicate that it is a weak interaction.

The analyzed parameters indicate that by increasing the charge (integers) of the Lewis acid, many un-quantized changes (continuous not integers) occur. The NPA-based group charge analysis illustrates that owing to the zwitterion formation, the Be1 and Al1 structures suffer from excessive bond polarization (with respect to 2-AA). This theoretical organic chemistry study represents the first fundamental information about the zwitterions of β-amino acids.

ACKNOWLEDGMENTS

We thank New Mexico State University-USA for an access to run some calculations. We also thank Al-Hussein Bin Talal University for supporting this research (research grant 78/2008).

REFERENCES

1. Brauer, B.; Chaban, G. M.; Gerber, R. B.; *Phys. Chem. Chem. Phys.* **2004**, *6*, 2543.
2. Benzi, C.; Cossi, M.; Barone, V.; *Phys. Chem. Chem. Phys.* **2004**, *6*, 2557.
3. Miller, T. F.; Clary, D. C.; *Phys. Chem. Chem. Phys.* **2004**, *6*, 2563.
4. Moision, R. M.; Armentrout, P. B.; *Phys. Chem. Chem. Phys.* **2004**, *6*, 2588.
5. Stearns, J. A.; Das, A.; Zwier, T. S.; *Phys. Chem. Chem. Phys.* **2004**, *6*, 2605.
6. Maris, A.; *Phys. Chem. Chem. Phys.* **2004**, *6*, 2611.
7. Nolting, D.; Marian, C.; Weinkauf, R.; *Phys. Chem. Chem. Phys.* **2004**, *6*, 2633.
8. Wiedemann, S.; Metsala, A.; Nolting, D.; Weinkauf, R.; *Phys. Chem. Chem. Phys.* **2004**, *6*, 2641.
9. Gerhards, M.; Unterberg, C.; Gerlach, A.; Jansen, A.; *Phys. Chem. Chem. Phys.* **2004**, *6*, 2682.
10. Chin, W.; Mons, M.; Dognon, J.; Piuzzi,F.; Tardivel, B.; Dimicoli, I.; *Phys. Chem. Chem. Phys.* **2004**, *6*, 2700.
11. Yang, Z.; Rodgers, M. T.; *Phys. Chem. Chem. Phys.* **2004**, *6*, 2749.
12. Morgado, C. A.; Pichugin, K. Y.; Adamowicz, L.; *Phys. Chem. Chem. Phys.* **2004**, *6*, 2758.
13. Sobolewski, A. L.; Domcke, W.; *Phys. Chem. Chem. Phys.* **2004**, *6*, 2763.
14. Baker, E. S.; Gidden, J.; Ferzoco, A.; Bowers, M. T.; *Phys. Chem. Chem. Phys.* **2004**, *6*, 2786.
15. Macleod, N. A.; Simons, J. P.; *Phys. Chem. Chem. Phys.* **2004**, *6*, 2821.
16. Price, W. D.; Jockusch, R. A.; Williams, E. R.; *J. Am. Chem. Soc.* **1997**, *119*, 11988.
17. Julian, R. R.; Hodyss, R.; Beauchamp, J. L.; *J. Am. Chem. Soc.* **2001**, *123*, 3577.
18. Wyttenbach, T.; Witt, M.; Bowers, M. T.; *J. Am. Chem. Soc.* **2000**, *122*, 3458.
19. Bertran, J.; Rodriguez-Santiago, L.; Sodupe, M. J.; *J. Phys. Chem. B* **1999**, *103*, 2310.
20. Jockusch, R. A.; William, P. D.; Williams, E. R.; *J. Phys. Chem. A* **1999**, *103*, 9266.
21. Cerda, B. A.; Wesdemiotis, C.; *Analyst* **2000**, *125*, 657.
22. Strittmatter, E. F.; Williams, E. R.; *J. Phys. Chem. A* **2000**, *104*, 6069.
23. Wyttenbach, T.; Witt, M.; Bowers, M. T.; *Int. J. Mass Spectrom.* **1999**, *182/183*, 243.
24. Remko, M.; Rode, B. M.; *J. Phys. Chem. A* **2006**, *110*, 1960.
25. Jockusch, R. A.; Lemoff, A.; Williams, E. R.; *J. Am. Chem. Soc.* **2001**, *123*, 12255.
26. Rogalewicz, F.; Ohanessian, G.; Gresh, H.; *J. Comput. Chem.* **2000**, *21*, 963.
27. Ai, H.; Bu, Y.; Chen, Z.; *J. Chem. Phys.* **2003**, *118*, 1761.
28. Ai, H. Bu, Y.; Han, K.; *J. Chem. Phys.* **2003**, *118*, 10973.
29. Liu, H.; Sun, J.; Yang, S.; *J. Phys. Chem. A* **2003**, *107*, 5681.
30. Li, P.; Bu, Y.; Ai, H.; *J. Phys. Chem. A* **2003**, *107*, 6419.
31. Mó, O.; Yáñez, M.; Alkorta, I.; Elguero, J.; *J. Chem. Theory Comput.* **2012**, *8*, 2293.
32. Groeger, D. In *Encyclopedia of Plant Physiology, vol. 8*; Springer: New York, 1980, p. 128.
33. Unterhalt, B.; *Deutsche Apotheker Zeitung* **1971**, *111*, 263.
34. Grundon, M. F., In *Alkaloids;* Academic Press, Waltham **1988**, *32*, 341.
35. Janiec, W.; Pietryka, B.; Staniewska, E.; Golek, A.; *Wiadomosci Lekarskie* **1985**, *38*, 1675.
36. Murao, S.; *Nippon Nogei Kagaku Kaishi* **1989**, *63*, 874.
37. Gray, A. In *Methods in Plant Biochemistry*; Bryant, J., eds.; Elsevier: Amsterdam, 1993, chap.8.
38. Niemann, G.; *J. Phytochem.* **1993**, *34*, 319.
39. Fuchs, Von J.; Milbradt, R.; *Dermatosen Beruf Umwelt* **1994**, *42*, 20.
40. Waterman, P. G.; *Biochem. Syst. Ecol.* **1999**, *27*, 395.
41. Ostrowski, S.; *Pol. J. Chem.* **2001**, *75*, 1661.
42. Avotinsh, F.; Petrova, M.; Strakovs, A.; *Rigas Tehniskas Universitates Zinatniskie Raksti, Serija 1: Materialzinatne un Lietiska Kimija* **2001**, *3*, 17.
43. Randhawa, G. S.; Hassani, R.; *Ind. J. Exp. Biol.* **2002**, *40*, 755.
44. Avendano, C.; Menendez, J. C.; *Curr. Org. Chem.* **2003**, *7*, 149.
45. Wiklund, P.; Bergman, J.; *Curr. Org. Synth.* **2006**, *3*, 379.
46. Nauen, R.; *Pest Manage. Sci.* **2006**, *62*, 690.
47. Tillequin, F.; *Phytochem. Rev.* **2007**, *6*, 65.
48. Harteneck, C.; Frenzel, H.; Kraft, R.; *Cardiovasc. Drug Rev.* **2007**, *25*, 61.
49. Genovese, S.; Curini, M.; Epifano, F.; *Phytochem.* **2009**, *70*, 1082.
50. Irshaidat, T.; *Asian J. Chem.* **2011**, *23*, 3243.
51. Irshaidat, T.; *Jordan J. Chem.* **2010**, *6*, 33.
52. Irshaidat, T.; *Mol. Simul.* **2011**, *37*, 414.
53. Irshaidat, T.; Saraireh, I. A. M.; Akintola, O.; *J. Chem. Soc. Pak.* **2012**, *34*, 815.
54. Becke, A. D.; *J. Chem. Phys.* **1993**, *98*, 5648.

55. Rassolov, V. A.; Ratner, M. A.; Pople, J. A.; Redfern, P. C.; Curtiss, L. A.; *J. Comput. Chem.* **2001**, *22*, 976.
56. McLean, A. D.; Chandler, G. S.; *J. Chem. Phys.* **1980**, *72*, 5639.
57. Krishnan, R.; Binkley, J. S.; Seeger, R.; Pople, J. A.; *J. Chem. Phys.* **1980**, *72*, 650.
58. Glendening, E. D.; Reed, A. E.; Carpenter, J. E.; Weinhold, F.; NBO version 3.1.
59. Wolinski, K.; Hilton, J. F.; Pulay, P.; *J. Am. Chem. Soc.* **1990**, *112*, 8251.
60. Frisch, M.; Trucks, G.; Schlegel, H.; Scuseria, G.; Robb, M.; Cheeseman, J.; Montagomery, J.; Verven, J. R.; Kudin, K.; Burant, J.; Iyenger, S.; Tomasi, J.; Barone, V.; Mennucci, B.; Cossi, M.; Scalmani, G.; Rega, N.; Petersson, G.; Nakatsuji, H.; Hada, M.; Toyota, K.; Fukuda, R.; Hasegawa, J.; Ishida, M.; Nakajima, T.; Honda, Y.; Kitao, O.; Nakai, H.; Klene, M.; Li, X.; Konx, J.; Hratchian, H.; cross, J.; Adamo, C.; Jaramillo, J.; Gomperts, R.; Stratmann, R.; Yazyev, O.; Austin, A.; Cammi. R.; Pomelli, C.; Ochterski, J.; Ayala, P.; Moromuka, K.; Voth, G.; salvador, P.; Dannenberg, J.; Zakrzewski, V.; Dapprich, S.; Daniels, A.; Strain, M.; Farkas, O.; Malick, D.; Rabuck, A.; raghavachari, K.; foresman, J.; Ortiz, J.; Cui, Q.; Baboul, A.; Clifford, S.; Cioslwski, J.; Setvanov, B.; Liu, G.; Liashenko, A.; Piskorz, P.; Komaromi, I.; Marton, R.; Fox, D.; Keith, T.; Al-Laham, M.; Peng, C.; Nanayakkara, A.; Challacombe, M.; Gill, P.; Johnson, B.; Chen, w.; Wong, M.; Gonzalez, C.; Pople, J.; *Gaussian 03, Revision E.1*, Gaussian, Inc., Pittsburgh PA 2003.
61. Krygowski, T. M.; *J. Chem. Inf. Comput. Sci.* **1993**, *33*, 70.
62. Jin, X.; Hu, B.; Jia, H.; Liu, Z.; Lu, C.; *Quim. Nova* **2014**, *37*, 74.
63. Romano, E.; Ladetto, M. F.; Brandán, S. A.; *Comput. Theor. Chem.* **2013**, *1011*, 57.
64. Vagánek, A.; Rimarčík, J.; Ilčin, M.; Škorňa, P.; Lukeš, V.; Klein, E.; *Comput. Theor. Chem.* **2013**, *1014*, 60.
65. Martínez, R. F.; Ávalos, M.; Babiano, R.; Cintas, P.; Light, M. E.; Jiménez, J. L.; Palacios, J. C.; *Tetrahedron* **2014**, *70*, 2319.
66. Afzali, R.; Vakili, M.; Tayyari, S. F.; Eshghi, H.; Nekoei, A. -R.; *Spectrochim. Acta, Part A* **2014**, *117*, 284.
67. Chipanina, N. N.; Oznobikhina, L. P.; Aksamentova, T. N.; Romanov, A. R.; Rulev, A. Y.; *Tetrahedron* **2014**, *70*, 1207.
68. Sridevi, C.; Velraj, G.; *Spectrochim. Acta, Part A* **2014**, *121*, 533.
69. Li, H.; Zhang, L.; Fan, X.; *Comput. Theor. Chem.* **2014**, *1032*, 90.
70. Saeed, A.; Khurshid, A.; Jasinski, J. P.; Pozzi, C. G.; Fantoni, A. C.; Erben, M. F.; *Chem. Phys.* **2014**, *431-432*, 39.
71. Szatyłowicz, H.; *J. Phys. Org. Chem.* **2008**, *21*, 897.
72. Grabowski, S. J.; *Chem. Rev.* **2011**, *111*, 2597.
73. Gilli, P.; Pretto, L.; Bertolasi, V.; Gilli, G.; *Acc. Chem. Res.* **2009**, *42*, 33.
74. Frisch, M. J.; Scheiner, A. C.; Schaefer III, H. F.; Binkley, J. S.; *J. Chem. Phys.* **1985**, *82*, 4194.
75. Dannenberg, J. J.; Rios, R.; *J. Phys. Chem.* **1994**, *98*, 6714.